Chemical Engineering Journal 166 (2011) 207–217

Contents lists available at ScienceDirect

Chemical Engineering Journal

journal homepage: www.elsevier.com/locate/cej

# Desulfurization of diesel fuels by selective adsorption on activated carbons: Competitive adsorption of polycyclic aromatic sulfur heterocycles and polycyclic aromatic hydrocarbons

Jie Bu, Gabriel Loh, Chuandayani Gunawan Gwie, Silvia Dewiyanti, Michael Tasrif, Armando Borgna*

*Institute of Chemical and Engineering Sciences (A*Star), 1 Pesek Road, Jurong Island, Singapore 627833, Singapore*

ARTICLE INFO

*Article history:*
Received 8 September 2010
Received in revised form 21 October 2010
Accepted 22 October 2010

*Keywords:*
Desulfurization of diesel
Selective adsorption
Activated carbon
Dibenzothiophene
Polyaromatic

ABSTRACT

Adsorptive affinity of polycyclic aromatic sulfur heterocycles (PASHs) and polycyclic aromatic hydrocarbons (PAHs) on activated carbons and the effect of PAHs on the adsorption performance of PASHs were studied. Adsorptions of real and model diesels (MDs) containing aromatics and sulfur compounds over several activated carbons were conducted in both batch and fixed-bed adsorption systems. The adsorption results showed that adsorptive affinities of molecules with polycyclic aromatic skeleton structure are primarily governed by the π–π dispersive interaction between the aromatic rings and the graphene layers of activated carbons. In addition, the electron donor–acceptor mechanism also plays an important role for S-containing molecules. Furthermore, for effective adsorption of large molecules, not only the pore size of the adsorbent should be, at least, larger than the critical diameter of the adsorbate, but also the pore size should also be sufficiently large to reduce diffusional resistance during adsorption. Based on this studies, it can be concluded that the adsorption selectivity increases as follows: naphthalene < fluorene < dibenzothiophene < 4,6-dimethyl dibenzothiophene < anthracene < phenanthrene. The adsorption capacity of PASHs decreases significantly in the presence of PAHs as result of the adsorption competition due to similar structure, molecular diameter and adsorption mechanisms.



## 1. Introduction

Desulfurization of transportation fuels such as diesel has increasingly gained importance since most of the countries, particularly the developed ones, have implemented more stringent legislation to regulate sulfur content of transportation fuels. The new regulations brought down the sulfur level of diesel from about 400 to 500 ppm (parts per million on weight basis) to 15 ppm. Near zero sulfur diesel fuel of 15 ppm or less allows advanced post engine exhaust clean up devices to effectively remove emissions and particulate matters. Due to the additional desulfurization process required for fuel refining, there has been a growing concern to the long term economics of petroleum refineries.

Currently, the common sulfur specification is 500 ppm in several countries; however, some countries have tighter specification. Ultra low sulfur diesel (ULSD) fuel of less than 50 ppm became the specification in both the European Union and Japan in 2005. The European Commission further adopted a 10 ppm sulfur specification for road diesel fuel beginning January 1, 2005 with full conversion by 2010. An U.S. EPA rule of 15 ppm sulfur highway diesel fuel was implemented on June 1, 2006 [1]. U.S. pipelines are anticipated to include a plan to deliver a sulfur level below 10 ppm fuel. In 2007, Japan proposed sulfur level of 10 ppm in their fuel. Several countries in other regions of the world are also working to reduce the sulfur content in diesel fuel. Conventional hydrodesulfurization (HDS) processes have been employed extensively by refineries to remove organic sulfur compounds from fuels for several decades and the lowest sulfur content achieved by such processes is around 500 ppm, although ULSD can be achieved using deep HDS. However, to meet the challenges of producing ultra-clean fuels with sulfur content lower than 15 ppm, both capital investment and operational costs would increase due to more severe operating conditions. Consequently, advanced desulfurization technologies such as ODS [2], and selective adsorption of organic sulfur compounds over various adsorbents [3–13] have been extensively investigated.

A sulfur adsorption at ambient temperature process was explored to achieve ultra clean diesel and gasoline by Song and Ma [14]. A 5 wt.% metal loaded on silica gel was used as an adsorbent for selective adsorption of sulfur. Other adsorption processes such as IRVAD and S-Zorb operates at high temperature, 240 °C and 340–410 °C, respectively [15,16]. Yang and coworkers [3,13] reported that Cu and Ag-exchanged Y-type zeolites were very effective in selective adsorption of thiophenes. These exchanged zeolites

* Corresponding author. Fax: +65 6316 6182.
*E-mail address:* Armando_borgna@ices.a-star.edu.sg (A. Borgna).

1385-8947/$ – see front matter © 2010 Elsevier B.V. All rights reserved.
doi:10.1016/j.cej.2010.10.063

can be regenerated by thermal treatments at 350 °C under flowing air.

Recently, activated carbons (AC) have been recognized and widely used as adsorbents in gas-phase and liquid-phase adsorptions for removal of organic sulfur compounds [8–12,17–22]. This is due to their very high surface areas, large pore volumes, and tunable surface properties by introducing functional groups. The specific surface areas and porosities of AC are greatly affected by the precursors of carbonaceous materials and the preparation methods. In most cases, activated carbons were used for the adsorption of compounds with weaker polarity from gas-phase or polar fluid-phase such as the adsorption of organics in wastewater. Thus, one of the main challenges for adsorptive desulfurization of liquid hydrocarbon fuels is to selectively separate the sulfur compounds of low polarity from a non-polar fluid phase [9]. In the Oxidative Desulfurization process, the sulfur compounds present in diesel are oxidized by the oxidizing agent to produce the corresponding sulfones [2]. The removal of the highly polar sulfones from diesel matrix by adsorption using AC could be a promising approach. Several recent studies have showed that some activated carbons can also have higher adsorption capacities for organic nitrogen compounds [8,12,23,24].

Organic sulfur compounds are abundant non-hydrocarbon constituents in petroleum. The sulfur content of petroleum fuels contributes to the formation of sulfur dioxide ($SO_2$), which causes both acid deposition and poisoning of the catalytic converters in vehicles. A large fraction of the organic sulfur in diesel fuels has aromatic structures, especially alkylated homologues of polycyclic aromatic sulfur heterocycles (PASHs). It was reported that benzothiophene (BT), dibenzothiophene (DBT) and their alkylated homologues are the most abundant organo-sulfur compounds in diesel fuels [25]. BT and DBT accounted for more than 50% of the total sulfur in diesel fuel, whereas the largest fraction of sulfur compounds present in low-sulfur diesel fuels are C2-DBTs such as 4,6-dimethyldibenzothiophene (4,6-DMDBT) [26]. Therefore, 4,6-DMDBT has to be included in the composition of model diesel (MD) for adsorption studies [4,8,9].

Diesel fuel not only contains organic sulfur compounds like PASHs but also a large fraction of aromatic compounds with similar structure to that of PASHs, which needs to be partly removed as well. In diesel fuels, the aromatics not only have direct impact on the emissions of particulates and poly-aromatic ring compounds, but also they have great influence on flame temperature which affects NOx formation. Higher aromatics content give rise to higher temperatures, resulting in increased NOx emissions. A reduction in total aromatic content from 30 to 10% significantly lowered NOx emission by 5% in light duty engines and by almost 4% in heavy duty engines. Typically, aromatic compounds in diesel are classified by the number of aromatic rings namely; mono-aromatic, di-aromatic, and tri-aromatic or polycyclic aromatic hydrocarbons (PAHs). Most diesels contains more PAHs than organic sulfur compounds [27,28]. Although it was found that activated carbons possess high adsorptive capacity to large PAHs molecules such as phenanthrene (PHE) and anthracene (AN) in both solutions [29–32] and organic solvents [33,34], the competitive adsorption of both PASHs and PAHs on ACs, especially, targeting desulfurization of diesel fuels was not sufficiently addressed.

One of the objectives of the present study is to investigate the adsorptive affinity of PASH and PAHs to activated carbons, as well as the effect of PAHs on the adsorption performance of PASH. Thus, the adsorption isotherm of PASH and PAHs were examined in both continuous fixed bed and batch adsorption system. The quantified properties of both the adsorbate and adsorbent were correlated with the adsorption performances to determine their relationships with adsorption selectivity and capacity.

In the present study, a number of activated carbons derived from different raw materials were applied for desulfurization by selective adsorption of real diesel in a fixed-bed flow system. A selected number of activated carbons were further examined in a batch adsorption system using model diesel. Surface acidity of the ACs was determined by using the classical Boehm's method.

## 2. Experimental

### 2.1. Carbon materials

All carbon materials used in this study are commercial activated carbons. AC1 was obtained from Kuraray Chemical Co. Ltd. (Japan), while AC2 to AC7 were obtained from Beijing Guanghua Wood (China). The structural characteristics of selected activated carbons were determined using nitrogen adsorption isotherms at 77 K. The textural and physical–chemical surface properties were correlated with the adsorption performance.

### 2.2. Characterization of carbon materials

Specific surface areas and pore volumes were determined by $N_2$ adsorption. An automated adsorption apparatus (Quantachrome, Autosorb-6B) was used. $N_2$ adsorption was carried out at liquid $N_2$ temperature (77 K). Prior to analysis, the samples were degassed at 150 °C in a vacuum system at about $10^{-4}$ Torr. The specific surface areas were calculated using the BET equation. The specific surface areas ($S_{BET}$) were determined using the Brunauer–Emmett–Teller (BET) method in the relative pressure range of 0.05–0.2. The micropore volumes ($V_{mi}$) were obtained with the accumulative pore volume using density-functional-theory (DFT) method. The total pore volumes ($V_{total}$) were obtained from the volumes of nitrogen adsorbed at a relative pressure of 0.95. The mesopore volumes ($V_{me}$) were calculated by subtracting $V_{mi}$ from $V_{total}$. The pore size distribution curves and cumulative pore volume plots were obtained using the DFT method [35].

### 2.3. Boehm titration

The oxygenated surface groups were determined according to the Boehm's method [26,36,37]. 1 g of activated carbon was placed in 25 mL of the following 0.05N solutions: sodium hydroxide, sodium carbonate, sodium bicarbonate, and hydrochloric acid, separately. The vials were sealed and shaken for 24 h and then 5 mL of each filtrate was pipetted and titrated with HCl or NaOH, according to the pH of the filtrate. The number of acidic sites was calculated under the assumption that NaOH neutralizes carboxyl, phenolic, and lactonic groups; $Na_2CO_3$ neutralizes carboxyl and lactonic; and $NaHCO_3$ neutralizes carboxyl groups. Lastly the number of surface basic sites was calculated from the amount of hydrochloric acid used.

### 2.4. Fourier transform infrared spectroscopy (FTIR)

FTIR spectra (4000–400 $cm^{-1}$) for different AC samples were recorded on a Nicolet Impact 410 FTIR spectrometer (Nicolet Instrument Corporation). The spectra of the samples were recorded in transmission mode using KBr wafers containing 0.5 wt% of carbon. These wafers were dried overnight at 120 °C before recording the spectra. The spectra were obtained by adding 64 scans with a resolution of 4 $cm^{-1}$.

### 2.5. Real diesel and model diesel

The diesel fuel used in this contribution was supplied by Singapore Refinery Co. Ltd. (SRC). The aromatics compositions

**Table 1**
Physical properties of activated carbons.

| Sample | Carbon source | $S_{Total}$ ($m^2/g$) | $S_{mi}$ ($m^2/g$) | $S_{me}$ ($m^2/g$) | $V_{total}$ ($cm^3/g$) | $V_{mi}$ ($cm^3/g$) | $V_{me}$ ($cm^3/g$) | $V_{me}$ (%) |
|---|---|---|---|---|---|---|---|---|
| AC1 | Pitch | 1403 | 1337 | 66 | 0.583 | 0.495 | 0.088 | 15.1 |
| AC2 | Apricot | 729 | 500 | 229 | 0.472 | 0.379 | 0.093 | 19.7 |
| AC3 | Apricot | 713 | 282 | 431 | 0.557 | 0.368 | 0.189 | 33.9 |
| AC4 | Apricot | 833 | 710 | 123 | 0.634 | 0.439 | 0.196 | 30.9 |
| AC5 | Apricot | 1020 | 596 | 424 | 0.734 | 0.526 | 0.208 | 28.3 |
| AC6 | Coconut | 986 | 525 | 461 | 0.801 | 0.501 | 0.300 | 37.4 |
| AC7 | Wood | 1100 | 750 | 350 | 1.061 | 0.499 | 0.561 | 52.9 |

of real diesels as provided by the supplier are shown in Table 2.

In addition, in order to compare adsorption selectivities, a MD was prepared by adding sulfur compounds such as 4,6-dimethyldibenzothiophene, and various mono-aromatic, di-aromatic and tri-aromatic compounds to hexadecane. A MD containing quinoline and 4,6-DMDBT was also prepared to investigate the adsorption capacity of nitrogen compounds and their competitive effects on the adsorption of sulfur. The total sulfur content of all prepared MDs was 400 ppmw. All compounds used to prepare MDs were purchased from Aldrich Chemical Co. and no further purification was carried out.

### 2.6. Adsorption of diesels in a fixed-bed adsorption system

Dynamic adsorption experiments were carried out by flowing diesel through a fixed bed adsorber at 75 °C in order to determine the adsorption capacity of the ACs. A packed-column was loaded with about 6–15 g of activated carbon with a particle size of 400–800 μm. The dimensions of the stainless steel adsorption column used were: 1 cm (diameter) × 33 cm (length). External electrical heating was supplied to the column to control the bed temperature. A number of activated carbons were tested. Adsorption experiments were carried out using a fixed volume of the adsorbent (26 $cm^3$) and a LHSV of 0.5 $h^{-1}$.

Once the adsorption process was started, samples of the product were collected at fixed time intervals. The sulfur content of the effluent was then analyzed using a Total Sulfur Analyzer (TS-100, Mitsubishi Chemical Co.). The analysis was carried out in accordance with the certified method; Oxidation Decomposition and Ultraviolet Fluorescence ASTM-D5453. A 6890 GC equipped with a G2350A atomic emission detection (AED) (Agilent Technologies, Palo Alto, CA, USA) was also used for quantifying sulfur components such as polycyclic aromatic sulfur heterocycles.

The aromatic hydrocarbons in diesel were analyzed using an Agilent 6890 GC/FID with HP-5 column according to the IP391-01 method to determine the concentration of mono-aromatic hydrocarbons (MAH), di-aromatic hydrocarbons (DAH), and tri- (TAH) or poly aromatic hydrocarbons (T + AH), prior and after to the adsorption process. The GC was equipped with a split/splitless injection port and operated in split mode.

### 2.7. Adsorption of model diesels in batch mode

Batch mode adsorption was conducted by contacting the MD containing individual sulfur compounds or one type of PAH with the adsorbents in a 20 mL bottle placed on a reciprocating shaker. After the desired adsorption time, the mixture of the treated MD and adsorbent was filtered, and the sulfur or PAH concentration in the treated MD was quantitatively analyzed to determine the adsorption capacity and selectivity of the adsorbents.

The amount adsorbed at equilibrium, $q_e$ (μmol/g), was calculated using the following equation:

$$q_e = \frac{(C_0 - C_e)W}{W_{AC}} \quad (1)$$

where $C_0$ and $C_e$ are the initial and equilibrium concentrations of adsorbate (μmol/g), respectively, $W$ (g) is the weight of the solution and $W_{AC}$ (g) is the mass of the adsorbent. $q_e$ (μmol/g) is the amount adsorbed at equilibrium concentration $C_e$ (μmol/g). The adsorption equilibrium data were fitted using the Langmuir equation:

$$\frac{C_e}{q_e} = \frac{1}{K_L q_m} + \frac{C_e}{q_m} \quad (2)$$

where $q_m$ (μmol/g) is the maximum adsorption capacity, $K_L$ (g/μmol) is the adsorption equilibrium constant, characteristic of the affinity between the adsorbent and adsorbate. $K_L$ and $q_m$ can be obtained by linear regression of ($C_e/q_e$) vs. $C_e$ data.

The adsorption data were also fitted using the Freundlich isotherms. The Freundlich isotherm is an empirical model that can be applied for non-ideal adsorption on heterogeneous surfaces as well as for multilayer adsorption. The Freundlich isotherm is given by Eq. (3), which correlates the adsorbed amount at the equilibrium, $q_e$ (μmol/g), to the equilibrium concentration, $C_e$ (μmol/g).

$$q_e = K_f {C_e}^{1/n} \quad (3)$$

where $K_f$ is the Freundlich adsorption constant ($(g/\mu mol)^{1/n}$), which is an indicator of the adsorption capacity, while n refers to the adsorption tendency. In all cases, a double-log plot of $q_e$ vs. $C_e$ data resulted in a good linear relationship, allowing for the estimation of the model parameters $K_f$ and $n$ by linear regression.

The total sulfur concentration of the initial and treated model diesels were analyzed using a Mitsubishi Chemical Co. TS-100 total sulfur analyzer. The instrument was calibrated in our laboratory in the range of 0–500 ppmw sulfur by diluting 5000 ppmw dibutylsulfide in toluene into several different concentrations. A linear calibration curve was obtained. The concentration of PAHs in the model diesel prior to and after the batch adsorption process were quantitatively analyzed using an Agilent 6890 gas chromatograph with HP-5 column connected to a flame ionization detector (GC-FID).

## 3. Results and discussion

The textural and physical characteristics of all ACs used in this work were determined using $N_2$ adsorption isotherms at 77 K. Table 1 summarizes the textural properties. The composition of the real diesel as provided by the supplier is shown in Table 2.

### 3.1. Adsorption capacity of various activated carbons

A numbers of activated carbons were screened using a fixed-bed adsorber as preciously described. The breakthrough curves for the adsorptive desulfurization of commercial diesel (SRC400) over several adsorbents are shown in Fig. 1.

**Table 2**
Composition of the real diesel fuel (SRC400).

| Organics in diesel | Concentration | | Method |
|---|---|---|---|
| | *S* (ppmw) | wt.% | |
| PASHs | 398 | ~0.26 | ASTM D5453-06 GC/AED |
| Mono aromatic hydrocarbons (MAH), wt% | | 30.9 | |
| Di-aromatic hydrocarbons (DAH), wt% | | 5.3 | IP 391/01 |
| Tri + aromatic hydrocarbons (TAH), wt% | | 1.4 | |
| Paraffins | | ~62.2 | GC/FID |

Note: GC/AED analysis showed that 4,6-DMDBT is the main PASH compound.

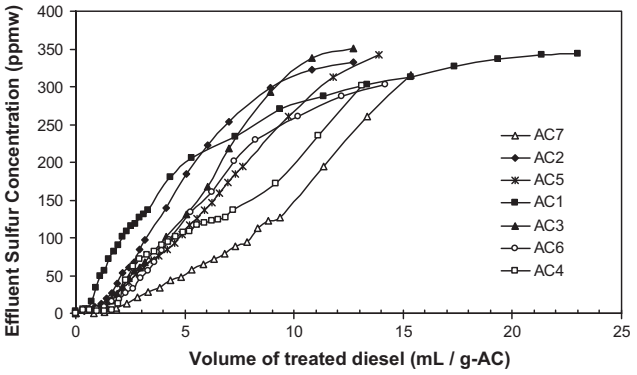


**Fig. 1.** Breakthrough curves for the adsorptive desulfurization of commercial SRC400 diesel over different activated carbons. Sulfur analysis data were obtained from total sulfur analyzer (TS-100).

The breakthrough curves shown in Fig. 1 clearly indicate that activated carbons derived from different raw materials and with different textural properties perform very differently in terms of adsorption of sulfur compounds in diesel. Activated carbons with large surface area, pore volume ($\geq$0.8 $cm^3/g$) and high mesopore volume ratio (ratio of mesopore volume to the total pore volume $\geq$50%) showed high adsorption capacity.

Based on the breakthrough curves, the sulfur adsorption capacity, $q$ (mg-S/g-AC), was calculated by performing a mass balance and integrating the corresponding breakthrough curves:

$$q = \frac{Q_{\text{fuel}} \cdot 10^{-3} \cdot C_0}{W_{\text{AC}}} \int_0^{t_{\text{end}}} [1 - \frac{C(t)}{C_0}]\, dt \quad (4)$$

where the $Q_{\text{fuel}}$ (g/min) is the diesel inlet flow rate; $W_{\text{AC}}$ (g) is the weight of adsorbent loaded into the fixed bed column; $C_0$ is the inlet sulfur concentration (400 S-ppmw); $C(t)$ is the sulfur concentration of the outlet stream. As expressed by Eq. (4), the area between the line $C(t)/C_0 = 1$ and the breakthrough curve of a given compound is proportional to the adsorption capacity $q$. In Fig. 1, the vertical axis represents the $S$ concentration of the effluent from the fixed-bed adsorber, which is proportional to $C(t)/C_0$, being $C_0$ 400 ppmw. For instance, when $C(t)/C_0 = 0.05$, the sulfur concentration of the effluent, $C(t)$, is about 20 ppmw of sulfur. Fig. 1 clearly shows that the adsorption capacity of the different activated carbons decreases as follows: AC7 > AC4 >AC 6 > AC3 > AC5 > AC2 > AC1.

The adsorption capacity can be estimated from the breakthrough curves at different effluent sulfur concentrations. When the effluent sulfur concentration of the real diesel reaches 300 ppmw, the adsorption capacity could be considered a close estimation of the maximum adsorption capacity since the adsorbent will be saturated when the effluent sulfur concentration reaches 400 ppmw. The relationship between the adsorption capacity at different effluent sulfur concentrations and the mesopore volume of various carbons is shown in Fig. 2.

The results reveal that activated carbons derived from biomass feedstocks such as wood (AC7) or apricot (AC4), show higher adsorption capacity than that of activated carbons derived from pitch (AC1). This is probably due to the larger surface area and higher percentage of mesopore volume of the activated carbons derived from biomass (Table 1). It can be seen from Fig. 2 that the higher the percentage of mesopore volume of the activated carbon, the higher the DBTs adsorption capacity. This suggests that DBTs adsorption capacity is primarily determined by the pore structure of the activated carbons, in good agreement with the observations reported by Yu et al. [17]. For the adsorption of large molecules such as DBT and 4,6-DMDBT, the adsorption capacity and the adsorption rate largely depend on the mesoporous volumes [19–22].

The adsorption of organic compounds onto natural adsorbents has been described as a complex process, mainly controlled by both chemical interactions and physical factors. The properties of the adsorbate molecules and the adsorbent, such as surface chemistry, specific surface areas and porosity often play critical roles.

Studies on the role of physical factors, especially molecular size, structure of polyaromatic compounds and pore structure of adsorbents, are relatively limited. Thus, the competitive effect of poly-aromatics with DBTs during adsorption was further investigated.

### 3.2. Effect of surface acidity on DBT adsorption

In order to get more insight into the adsorption performance of carbon materials of DBTs in MD, three typical activated carbons, AC1, AC4, and AC7, derived from different carbon sources, were selected and their surface chemical properties were examined in details. The quantification of the acid surface groups of these three AC samples is summarized in Table 3. The adsorption capacity of 4,6-DMDBT using a MD consisting of 400 ppmw of sulfur and 20 wt% of n-hexylbenzene dissolved in hexadecane was deter-

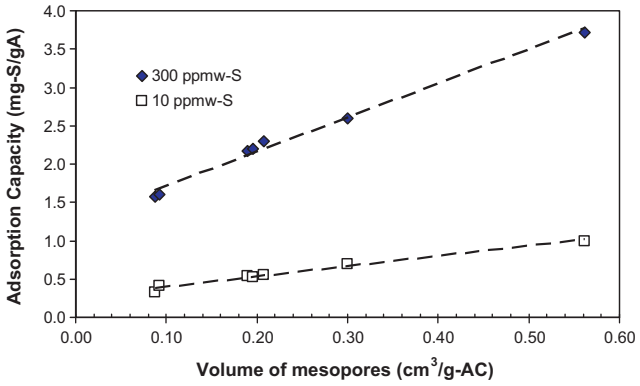


**Fig. 2.** Adsorption capacity of sulfur vs. mesopore volume of various activated carbons obtained at different effluent sulfur concentrations ($S$ = 10 and 300 ppmw).

**Table 3**
Quantification of acid surface groups on activated carbons and their adsorption capacities for 4,6-DMDBT.

| Adsorbent | $S_{BET}$ ($m^2/g$) | Surface acidity ($mmol/m^2 \times 10^4$) | | | | Equilibrium capacity at 400 ppmw of S[a] ($mg\text{-}S/m^2 \times 10^4$) |
|---|---|---|---|---|---|---|
| | | Carboxyl | Lactonic | Phenol | Total acidity | |
| AC1 | 1403 | 0.36 | 2.28 | 3.21 | 5.84 | 39.91 |
| AC4 | 833 | 7.21 | 2.28 | 2.02 | 11.51 | 97.28 |
| AC7 | 1100 | 9.77 | 2.27 | 2.27 | 14.32 | 122.73 |

[a] Measured by adsorption of model diesel containing 4,6-DMDBT (400 ppmw S) in batch adsorption mode.

mined. The adsorption capacities based on unit of surface area are also reported in Table 3.

From Table 3, it is evident that the adsorption capacity per unit of surface area depends on the density of carboxylic group on the surface. The adsorption capacity is significantly increased as the density of carboxyl functional groups increases [10,11,17,18].

Fig. 3 shows the FT-IR spectra of these ACs. Four bands at 1718, 1578, 1400, and 1138 $cm^{-1}$ were observed. The 1718 $cm^{-1}$ band is characteristic of stretching vibrations of carbonyl group C=O in carboxylic groups. The strong band at 1578 $cm^{-1}$ and the weak one at 1400 $cm^{-1}$ can be ascribed to asymmetric and symmetric $COO^-$ vibration, respectively [38]. The 1138 $cm^{-1}$ band may be attributed to both C–O stretching and O–H bending modes in phenolic and carboxylic groups [38,39]. AC7 spectra showed higher intensity at 1718 and 1578 $cm^{-1}$ as compared to the two other ACs, suggesting that AC7 has higher surface density of carboxylic groups than AC4 and AC1. This is also consistent with the Boehm titration results (Table 3).

The density of the acidic function groups on the carbon surface has a significant role in improving the adsorption capacity of DBTs. Electron-withdrawing groups such as electron acceptor sites and carboxylic groups are complementary to the electron pair donor sulfur atoms of DBTs, having two unpaired electrons [17]. As a consequence, electron donor–acceptor complexes would be formed [17]. This explains that the modification of activated carbon surfaces by thermal oxidation [17] or acid treatments [10,11,18] to increase the amount of acid functional groups on the surface usually results in an increase of adsorption of sulfur-containing compounds.

### 3.3. Adsorption isotherms of aromatic compounds and DBTs on ACs

Diesel fuels not only contain organic sulfur compounds such as dibenzothiophene, 4,6-DMDBT, but also a large amount of PAH compounds having aromatic structures similar to the one of PASHs. Thus the competitive adsorption between PAHs and PASHs might occur. In order to better understand the adsorptive affinity of PAHs and PASHs to activated carbon, the adsorption of several organic compounds – DBT, 4,6-DMDBT, anthracene, phenanthrene, fluorine (FLU), and naphthalene (NA) – on AC7 was studied in batch mode. The adsorption capacities as a function of the equilibrium concentrations of each adsorbate in the liquid phase are shown in Fig. 4, indicating that the adsorption capacity increases as the equilibrium concentration of the adsorbate in the liquid phase is increased.

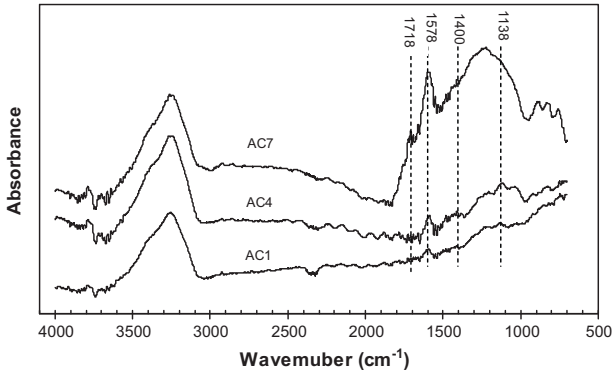


**Fig. 3.** FT-IR spectra of selected ACs.

Langmuir adsorption isotherm would yield a linear plot of $C_e/q_e$ versus $C_e$, where $C_e$ and $q_e$ are the concentrations of adsorbate in the liquid phase and the adsorbed phase at equilibrium, respectively. $K_L$ is the adsorption equilibrium constant. The maximum adsorption capacity, corresponding to the saturation coverage of the surface by the adsorbate, is represented by $q_m$. It is obvious that the Langmuir equation is not able to properly describe the adsorption isotherm data over the entire concentration range. As previously reported by Richard and Richard [32], two linear forms of the Langmuir equation were employed to determine the adsorption parameters for the adsorption of PAHs onto activated carbon from a liquid phase.

The fitting parameters for both the Langmuir and Freundlich isotherms are summarized in Table 4. The use of two linear regressions of the Langmuir equation allows us to obtain excellent fittings of the experimental data in the whole range. The plots of $C_e/q_e$ versus $C_e$ for six different adsorbates are shown in Fig. 5.

A good linear relationship between $C_e/q_e$ and $C_e$ was obtained in all cases. The parameters of the Langmuir isotherm determined from the linear range for values of $C_e$ greater than about 3 μmol/g-MD (100 ppmw of S) indicate that the adsorption equilibrium constant of tri-aromatics (PHE and AN) are similar to those of sulfur-containing compounds (DBT and 4,6-DMDBT). The parameters of the Langmuir isotherm determined from the experimental data at low $C_e$ are well fitted, but underestimated capacity at higher $C_e$ (see Table 4). As shown later, these observations may be due to different trends in relative adsorption at high and low relative concentration regions of the isotherms. Therefore, it is instructive to consider the relative adsorption in both ranges.

As shown in Table 4, the Langmuir parameters ($K_L$ and $q_m$) of 4,6-DMDBT, PHE and AN, which reflect the adsorptive affinity of these

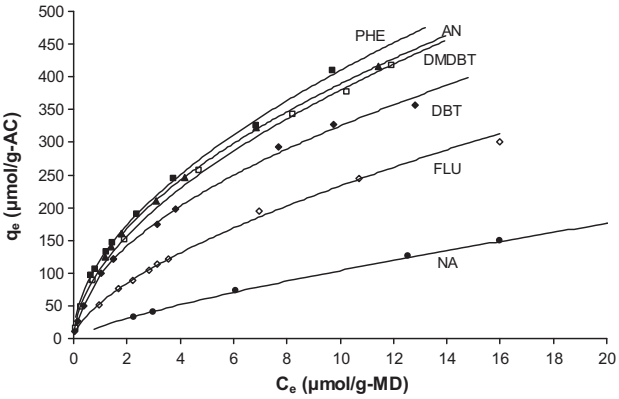


**Fig. 4.** Adsorption isotherms of different adsorbates on activated carbon AC7 at 303 K. Experimental data points (symbols) along with data fit according to the Langmuir isotherm equation (solid lines).

**Table 4**
Summary of the isotherm parameters.

| Adsorbate | Langmuir | | | | | | Freundlich | | |
|---|---|---|---|---|---|---|---|---|---|
| | For high $C_e$ | | | For low $C_e$ | | | $K_f$ (g/μmol)$^{1/n}$ | $1/n$ | $R^2$ |
| | $K_L$ (g/μmol) | $q_m$ (μmol/g) | $R^2$ | $K_L$ (g/μmol) | $q_m$ (μmol/g) | $R^2$ | | | |
| PHE | 0.159 | 666.7 | 0.975 | 0.810 | 303.0 | 0.985 | 119.40 | 0.534 | 0.999 |
| AN | 0.148 | 666.7 | 0.983 | 0.795 | 301.0 | 0.998 | 114.89 | 0.535 | 0.999 |
| 4,6-DMDBT | 0.157 | 625.0 | 0.989 | 1.000 | 227.3 | 0.991 | 97.72 | 0.606 | 0.995 |
| DBT | 0.149 | 555.6 | 0.990 | 0.843 | 232.6 | 0.970 | 85.80 | 0.608 | 0.995 |
| FLU | 0.090 | 500.0 | 0.990 | 0.276 | 238.1 | 0.980 | 54.40 | 0.632 | 0.998 |
| NA | 0.035 | 434.8 | 0.950 | 0.035 | 434.8 | 0.950 | 18.01 | 0.761 | 0.999 |

compounds to the activated carbon, are not significantly different in the high concentration region ($C_e$ > 3 μmol/g-MD). For instance, an organic liquid containing 400 ppmw of sulfur as 4,6-DMDBT has a $C_e$ value of 12.5 μmol/g-MD. At the same time, the values of the equilibrium adsorption capacity ($q_e$) of 4,6-DMDBT, PHE and AN are 88, 79, and 77 mg/g-AC, respectively. This suggests that a strong competitive adsorption between DBTs and PHE or AN could occur during the adsorption process under real conditions. Real diesel fuels usually consist of significantly larger percentage of polycyclic aromatic hydrocarbons as compared to DBTs (Table 2). Thus, it is important to investigate and understand the adsorptive affinity of PAH on AC surface and its effects on the adsorption selectivity as compared to DBTs.

The plots of $C_e/q_e$ versus $C_e$ of those compounds with similar aromatic structures are presented in Fig. 5, while Fig. 6 shows the magnitude of the product of $K_L$ and $q_m$ for each adsorbate in the range of $C_e$ > 3 μmol/g-MD, being this product a characteristic constant related to the strength of the adsorption which reflects the affinity of each adsorbate to the adsorbent [40]. Furthermore, as summarized in Table 4, the Freundlich isotherm allows us to obtain excellent fittings of the experimental data in the whole range. The $K_f$ values, which reflect the adsorption capacity, decrease as follows: PHE > AN > DMDBT > DBT > FLU > NA. In summary, the values of both the parameter ($K_L q_m$) from the Langmuir isotherm and the parameter $K_f$ from the Freundlich one clearly indicate that the adsorptive affinity of the adsorbates follows the order: PHE > AN > DMDBT > DBT > FLU > NA.

The DBT molecule, a three-ring aromatics with a sulfur atom, has stronger affinity than FLU, an equivalent three-ring structure [33]. The two unpaired electrons of the sulfur atom in DBT act as an electron donor to carboxylic groups (on the surface of AC); the electron-withdrawing groups acting as an electron acceptor [17]. However, the sulfur atom alone might not play a determining role in the adsorptive affinity of adsorbates to the surface of AC. We have found that the adsorptive affinity of PHE is even higher than DBT and 4,6-DMDBT. Many research groups reported a high adsorption capacity of AC in PAHs removal [29–34,36,41,42]. The interaction between adsorbate and adsorbent is favoured by the similar chemical behaviour of the surface and the adsorbate [43]; the dispersive interactions between the π electrons of the benzene rings in PAH and the electron rich region in the graphene layers could play an important role in the adsorptive affinity of these adsorbates to activated carbon [17,31,33,37,41]. Soscun and coworks recently reported that despite DBT has a static polarizability close to that of the anthracene molecule, the electric deformability of the sulfur compound is lower than the one of the three fused ring hydrocarbons, suggesting a bigger contribution of the delocalized π electrons in the tri-aromatic hydrocarbon than in the case of the S-containing compound [44]. It was also reported that the PAHs are able to form π–π complex between π-electrons of benzene rings and active sites on an activated carbon surface [33]. Therefore, it could be proposed that not only the donor–acceptor mechanism, but also the π–π dispersive interactions between the aromatic ring in PAHs and the graphene layers on AC are the key parameters to determine the adsorptive affinity of those molecules with polycyclic aromatic skeleton structure. This can explain that the molecules with three-aromatic rings (PHE, AN, 4,6-DMDBT, DBT and FLU) showed a significantly higher adsorptive affinity than two-ring aromatics (NA).

The $K_L$ $q_m$ of 4,6-DMDBT is higher as compared to DBT due to the presence of methyl substituent which are electron donors to the aromatic rings, leading to an increase of π-electron density on the aromatic rings and, thus, enhancing the adsorption affinity [8,9,37]. The higher affinity of PHE as compared to 4,6-DMDBT suggests the contribution of π–π dispersive interactions due to the three benzene rings of PHE to the adsorption affinity could be more dominant than the combined effects of dispersive interactions (due to the two benzene rings and one pentagonal ring) and the electron donor–acceptor interaction due to sulfur atoms in 4,6-DMDBT under our adsorption conditions. This phenomena is also

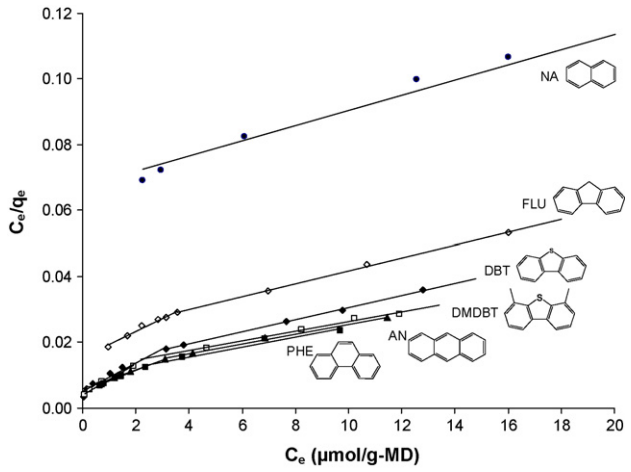


**Fig. 5.** Plots of the parameter $C_e/q_e$ vs. $C_e$ of various PAHs and PASHs.

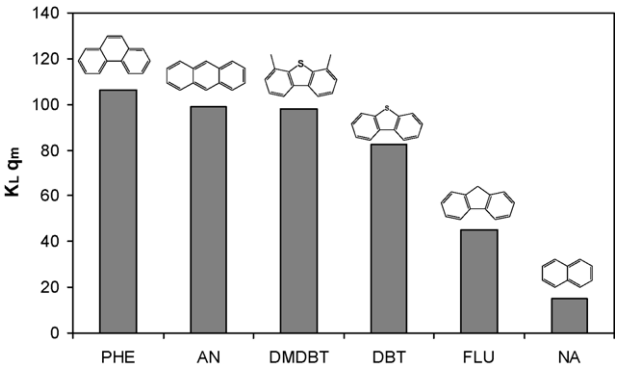


**Fig. 6.** $K_L \cdot q_m$ values of various PAHs and PASHs.

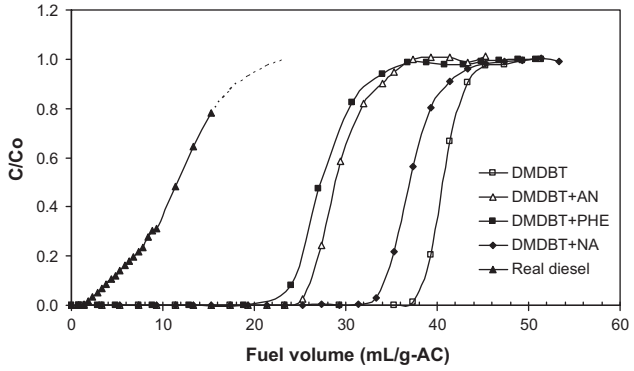


**Fig. 7.** Breakthrough curves of 4,6-DMDBT for Run-1 to Run-4 and real diesel.

encountered in the benzothiophene (BT)-naphthalene system [9]. The higher adsorption selectivity of activated carbon for NA than BT (both being two-ring aromatic compounds) indicates that in two-ring aromatics the electron donor–acceptor interaction of the sulfur atom alone may not be the only factor determining the adsorptive affinity.

Based on this study on the adsorption affinity of various adsorbates (Figs. 4–6), it can be concluded that the adsorption selectivity of these adsorbates increases in the following order: NA < FLU < DBT < 4,6-DMDBT < AN ≤ PHE. This was further investigated in a continuous fixed-bed adsorption system.

### 3.4. Adsorption experiments on activated carbons in a fixed-bed column

In order to study the adsorption performance of activated carbons, four experiments (Run-1 to Run-4) were carried out using MD in a fixed bed column packed with AC7 at 25 °C and employing a liquid hourly space velocity (LHSV) of 0.5 $h^{-1}$. The model diesel composition was of 0.265% of 4,6-DMDBT (400 ppmw of sulfur), 20 wt% of n-heptylbenzene, varying quantities of PAHs and hexadecane as balance. The compositions of the MDs used in the four experiments are listed in Table 5.

The breakthrough curves of sulfur for all experiments, Run-1 to Run-4, are shown in Fig. 7, revealing the effect of PAHs – naphthalene, anthracene or phenanthrene – on the sulfur adsorption capacity of AC7. In the case of MD without PAHs (Run-1), the activated carbon exhibits a high adsorption capacity for 4,6-DMDBT. The maximum adsorption capacity is 13.1 mg-S/g-AC, which corresponds to 0.4 mmol/g-AC. This is in agreement with the equilibrium adsorption capacity at 400 ppmw of sulfur of 0.41 mmol/g-AC (13.3 mg-S/g-AC), measured in batch mode (Fig. 4). However, in the presence of NA (Run-2), AN (Run-3) or PHE (Run-4), the adsorption capacity of AC7 for 4,6-DMDBT is significantly reduced. It can be seen that the presence of three benzene-ring aromatics (PHE and AN) has a much larger effect on the adsorption capacity of 4,6-DMDBT as compared to the two-ring aromatics (NA). Fig. 8(a) and (b) shows the breakthrough curves for the different components in the MDs containing AN and PHE (Run-3 and Run-4). The breakthrough curves of AN and PHE are similar to the one of 4,6-DMDBT. However, the adsorption capacity of the AC for PHE is significantly larger than AN. Both AN and PHE have larger adsorption capacity than 4,6-DMDBT. These findings are in agreement with the values of the adsorptive affinity of PHE, AN and DMDBT measured in batch experiments, which indicate that the affinity or adsorption selectivity increases in the order of NA < 4,6-DMDBT < AN < PHE.

The adsorption capacity of 4,6-DMDBT is much higher than NA. It is interesting to stress that, after passing through the saturation point ($C/C_0 = 1$), the outlet concentration of NA is higher than

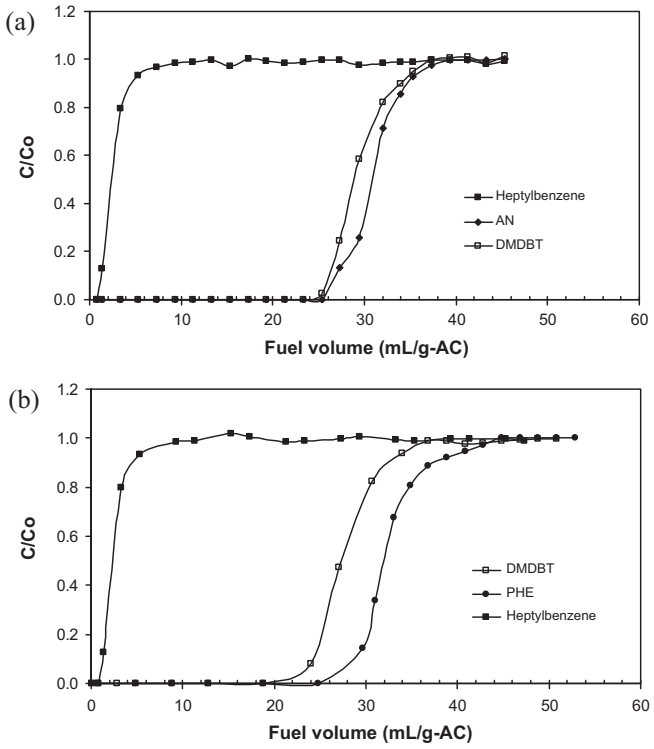


**Fig. 8.** (a) Breakthrough curves of Heptylbenzene, Anthracene and 4,6-DMDBT (Run-3). (b) Breakthrough curves of Heptylbenzene, Anthracene and 4,6-DMDBT (Run-4).

the original concentration in the model diesel ($C/C_0 > 1$), as clearly shown by Fig. 9. Then, it decreases gradually back to the initial concentration as the normalised concentration of 4,6-DMDBT increases to $C/C_0 = 1$. Therefore, it can be inferred that: (1) the adsorption of NA is at least partially reversible; (2) NA has much lower adsorptive affinity than 4,6-DMDBT, which results in a partial displacement of NA [8].

In Fig. 9, the area between the breakthrough curve of a given compound and line $C/C_0 = 1$, integrated between time 0 and before the saturation point, represents the amount of the adsorbed molecules, while the area between the breakthrough curve and the line $C/C_0 = 1$ after the saturation point represents the amount of molecules displaced. These results suggest that the adsorption competition between 4,6-DMDBT and PAHs is indeed taking place and this phenomena is particularly dominant in the presence of three-ring aromatics, resulting in a significant decrease of the adsorption capacity of 4,6-DMDBT.

### 3.5. Adsorption of real diesel on activated carbons in a fixed-bed packed column

Based on the results obtained from the adsorption experiments using model diesel both in batch and in flow mode, it can be concluded that the donor–acceptor mechanism for sulfur compound and the π–π dispersive interaction between the aromatic ring of PAHs and the graphene layers of AC are the key factors determining the adsorptive affinity of the adsorbates. It was later determined that adsorption of 4,6-DMDBT in the presence of both PAH (PHE or AN), which have similar polycyclic aromatic skeleton structure and, therefore, similar adsorptive affinity to activated carbon, resulted in the adsorption competition between the S-containing compound and the tri-aromatics.

It is important to stress that the PAH concentration (5 wt% of di-aromatics, and 1.4 wt% of tri-aromatics) in real diesel is about

**Table 5**
Composition of MD containing PAHs.

| Chemicals | Run-1 | | Run-2 | | Run-3 | | Run-4 | |
|---|---|---|---|---|---|---|---|---|
| | wt% | μmol/g | wt% | μmol/g | wt% | μmol/g | wt% | μmol/g |
| Hexadecane | 79.74 | | 79.58 | | 79.54 | | 79.51 | |
| n-Heptylbenzene | 20 | 1233.5 | 20 | 1233.5 | 20 | 1233.5 | 20 | 1233.5 |
| 4,6-DMDBT[a] | 0.27 | 12.5 | 0.27 | 12.5 | 0.27 | 12.5 | 0.27 | 12.5 |
| NA | – | – | 0.16 | 12.5 | – | – | – | – |
| AN | – | – | – | – | 0.20 | 12.5 | – | – |
| PHE | – | – | – | – | – | – | 0.22 | 12.5 |

[a] 4,6-DMDBT corresponds to 400 ppmw sulfur.

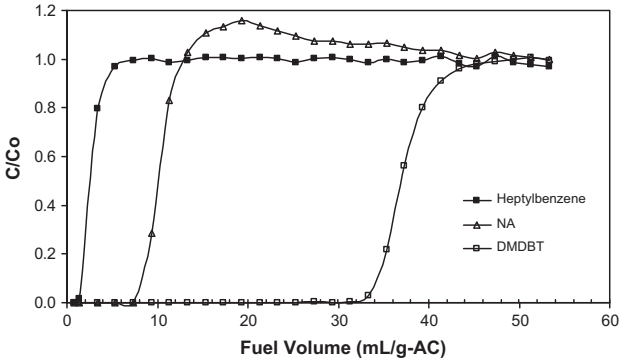


**Fig. 9.** Breakthrough curves of Heptylbenzene, Naphthalene and 4,6-DMDBT for Run-2.

six times higher than that of sulfur compounds (400 ppmw-S, Table 2). DBT, a relatively large molecule, can cover an area as large as $8 \times 12$ Å$^2$ [45], and the critical diameters of DBT and 4,6-DMDBT have been reported to be 8 and 9 Å, respectively [46,47]. PAH molecules such as phenanthrene, Anthracene or Fluorene have similar molecular size as compared to DBT. The molecular dimensions of various PAHs are also summarized in Table 6 [48].

Dubinin et al. [49] has proposed that the porous structure of activated carbon is tri-dispersed, consisting of micro-, meso-, and macropores. According to Dubinin, each of these groups of pores plays a specific role in the adsorption process. The porous structure of activated carbon can be envisaged as consisting of macropores which open up directly to the external surface, mesopores (transitional pore) which branch off from the macropores, and the micropores, which in turn branch off from the mesopores. Generally, the micropores contribute with the larger fraction of surface area and pore volume. Therefore, the micropores determine the adsorption capacity of a given activated carbon to a considerable extent. However, during adsorption of adsorbates with large molecular size, the access to the micropores of the adsorbent is limited [41,50]. Diffusion resistance is expected to be significant when the critical diameter of the adsorbate is comparable to the micropore size. Several studies reported that the diffusivity is reduced by the size restriction factor, the ratio of the critical solute diameter to the pore size [51,52]. In such situation, the macropores act as the primary transport channels, enabling adsorbate molecules to enter rapidly to smaller pores. As such, to a certain extent, the mesopores also play important role in determining the adsorption process and controlling the kinetics of the adsorption process [18,40,53].

Recently, Mastral and co-workers studied the adsorption of phenanthrene on different activated carbons. They reported that during the adsorption of phenanthrene, there are significant kinetic restrictions for the diffusion of the adsorbate in carbons with narrow microporosity, especially those of pore size close to the adsorbate molecular size [42]. For a real diesel containing relative high concentrations of large molecules, PAH and DBTs, the adsorption capacity is primarily determined by the pore structure of activated carbons, which has been described in Section 3.1 (Fig. 2).

Fig. 10 shows the pore size distribution of three typical activated carbons used in this work. AC1, AC4, and AC7 exhibit micropores, mesopores, and a mixture of micropores and mesopores, respectively (see Table 1). AC7 has the highest mesoporosity whereas AC1 shows the lowest. It can also be seen that AC1 has a bimodal pore distribution with pore sizes smaller than 8 Å and pore between 8 and 40 Å. AC4 and AC7 have a wider uni-modal pore size distribution with a significant pore volume between 8–40 Å, and 8–50 Å, respectively, in which adsorption of both DBTs and PAHs is favoured. The detailed characteristics of the pore structure of the activated carbons are shown in Table 7. During the adsorption of DBT, which has a critical diameter of about 8 Å, only the micropores with pore size larger than 8 Å are effective. From Fig. 10 (inset) and Table 7, the effective pore volume and surface area of AC1 available for the adsorption process is only about 50% of total volume and less than 30% of total surface area.

**Table 6**
Molecular sizes of various PAHs [48].

| PAH | Structure | Width (Å) | Length (Å) | Thickness (Å) |
|---|---|---|---|---|
| Naphthalene (NA) | 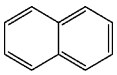 | 7.428 | 9.195 | 3.884 |
| Fluorene (FLU) | 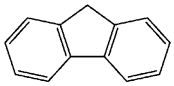 | 7.521 | 11.431 | 4.241 |
| Anthracene (AN) | 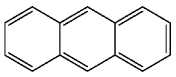 | 7.439 | 11.651 | 3.882 |
| Phenanthrene (PHE) | 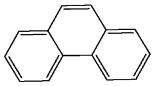 | 8.031 | 11.752 | 3.888 |

**Table 7**
Structural parameters of selected ACs calculated from $N_2$ adsorption/desorption isotherms and their adsorption capacities using real diesel.

| Sample | $S_{DFT}$ m²/g | $S$ > 8 Å m²/g/($S$%) | $S$ > 20 Å m²/g/($S$%) | $V_t$ cm³/g | $V$ > 8 Å m³/g/($V$%) | $V$ > 20 Å m³/g/($V$%) | Adsorbed amount of $S$ (mg-$S$/g-AC) |
|---|---|---|---|---|---|---|---|
| AC1 | 1403 | 379/(27%) | 66/(5%) | 0.583 | 0.30/(52%) | 0.09/(15%) | 1.8 |
| AC4 | 833 | 759/(91%) | 123/(15%) | 0.634 | 0.61/(96%) | 0.20/(31%) | 2.3 |
| AC7 | 1100 | 1052/(96%) | 350/(32%) | 1.061 | 1.05/(99%) | 0.56/(53%) | 3.7 |

*Note*: The adsorption capacity is based on the breakthrough curves shown in Fig. 11, corresponding to an effluent $S$ concentration = 300 ppmw $S$ ($C/C_0$ = 0.75).

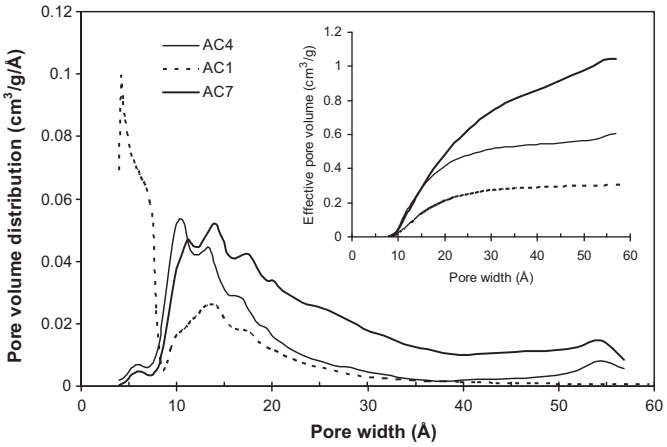


**Fig. 10.** DFT pore size distribution and effective pore volume (inset).

Fig. 11 shows the breakthrough curves for adsorption of total sulfur in real diesel (SRC400) in a fixed-bed column. In terms of adsorption performance, AC1 has the lowest adsorption capacity, followed by AC4 and AC7. This can be explained by the pore structure parameters of these ACs, obtained from the BET analysis shown in Fig. 10 and Table 7. The surface area of the ACs in the micropore range with pore sizes larger than 8 Å increases in the following order: AC1 < AC4 < AC7.

AC4 has a narrower pore size distribution than AC7 in the range of pore sizes > 8 Å, which may result in a higher diffusion resistance for large adsorbate molecules during adsorption. Studying the adsorption of DBT on carbon materials, Jayne et al. found that DBT molecules have kinetic restrictions for the diffusion into the pores with pore sizes in the range of 10–20 Å since the adsorption process requires a long time to reach the equilibrium [40]. Therefore, it could be proposed that, for effective adsorption of large molecules, not only the micropore size should be, at least, larger than the critical diameter of adsorbate, but also the pore size distribution should also be wide enough to minimize the kinetic diffusion resistance during the adsorption process. In line with this, it has been suggested that mesopores with pore sizes > 20 Å are also important to the adsorption process [18,40,53]. Valderrama et al. suggested that the mesopores of activated carbon may be as important as micropores when high molecular-weight compounds are present [29]. More recently, Bandosz and co-worker reported that acidic groups located on larger pores are critical for adsorption of DBT and 4,6-DMDBT [53]. They found that pores with sizes between 10 Å and 30 Å are very active in the adsorption process in spite of having a much smaller adsorption potential. Therefore, it has been proposed that acid functional groups located on those pores has high affinity to DBT and 4,6-DMDBT, resulting in an increase of the adsorption capacity.

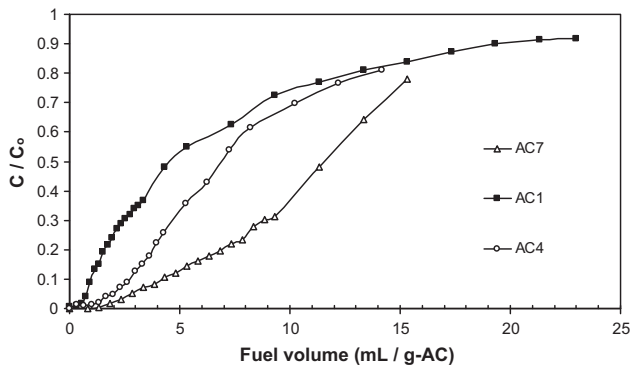


**Fig. 11.** Breakthrough curves of total sulfur during adsorption of a 400 ppm S commercial diesel (SRC400).

Besides ACs, other materials such as pi-complexation sorbents have also been reported in literature for desulfurization processes, exhibiting an outstanding adsorption capacity. For instance, an adsorption capacity of ca. 14 mg-S/g-A can be estimated from the literature for Cu exchanged Y zeolites [4,5,13], while a maximum adsorption capacity of ca. 4 mg-S/g-A was achieved in this contribution. Although a lower adsorption capacity is usually achieved using AC sorbents, these materials can still be considered as promising candidates for desulfurization processes, mainly because of their low cost and relatively facile regeneration. Recently, we have reported that thermal treatments can be successfully applied to fully recover the adsorption capacity of ACs after adsorbing S-containing compounds [54]. Furthermore, ACs can also be regenerated using a solvent-washing process [55].

In summary, the mesoporosity of activated carbons plays a key role in determining the adsorption capacity of S-containing compounds. The fraction of mesopores has to be carefully tuned in order to achieve an acceptable adsorption capacity. In addition, surface functional groups may enhance the adsorption capacity, but only when they are located in pores that are big enough to be accessible to the adsorbates.

## 4. Conclusions

Adsorptions of real and model diesel fuels containing aromatics and sulfur compounds over several activated carbons were conducted in both batch and fixed-bed continuous adsorption systems. The adsorption results provided a new insight into the adsorptive affinity of PASHs and PAHs to the activated carbons, as well as the effect of PAHs on the adsorption performance of PASHs.

The adsorptive affinity of those molecules having polycyclic aromatic skeleton structure is primarily governed by the π–π dispersive interaction between aromatic ring and graphene of activated carbon. In addition, the electron donor–acceptor mechanism also plays an important role for S-containing compounds. The contribution to the adsorption affinity of the π–π dispersive interactions due to the benzene rings of PAHs is more dominant than the combined effects of dispersive interactions (due to benzene rings and pentagonal ring) and the electron donor–acceptor interaction due to sulfur atoms.

Furthermore, both batch and fixed-bed continuous adsorption experiments also reveal that for effective adsorption of large molecules, not only the micropore size of adsorbent should be, at least, larger than the critical diameter of adsorbate, but also the pore size distribution should also be sufficiently wide to reduce the diffusion kinetic resistance during the adsorption process. The wider

the pores size distribution, the lower the kinetic restrictions for PASHs adsorption and, therefore, the higher the effective diffusion coefficient. This effect has been clearly shown by the experimental results, indicating that mesoporous activated carbons have significantly larger adsorption capacity as compared to microporous activated carbon. As polycyclic aromatic compounds such as PASHs and PAHs have similar critical molecular diameter, the effect of pore size distribution of activated carbon on the kinetic restrictions for the diffusion of adsorbates can be assumed to be also applicable to PASHs. Based on this studies, it can be concluded that the adsorption selectivity of several adsorbates increase in the following order: NA < FLU < DBT < 4,6-DMDBT < AN < PHE.

Due to the similar structure, critical molecular diameter and adsorption mechanisms, PAHs and PASHs showed comparable adsorptive affinity to activated carbon, resulting in adsorption competition between them. This competitive adsorption due to the presence of PAHs will be dominant when a real diesel is used as feedstock since it contains a much higher amount of PAHs as compared to PASHs. As a result, the adsorption capacity of PASHs decreases significantly in the presence of PAHs.

The present study allows us to get more insights into the key factors that govern the adsorption mechanisms of PASHs and PAHs, their adsorption competition, and the effects of diffusion kinetic restrictions arising from the pore size and size distribution of activated carbons. Thus, it is clear that the removal of organic sulfur compounds from real diesel using adsorption on activated carbons is a highly complex process. Therefore, an in-depth understanding of the adsorption competition between the DBTs and the aromatic compounds is crucial for the development of a cost-effective and sustainable desulfurization process.

## Acknowledgements

The authors are grateful to Dr. P.K. Wong and Dr. Keith Carpenter for providing constructive comments to this study. The authors also gratefully acknowledge the financial support from ETPL (A*STAR – Singapore).

## References

[1] Heavy-Duty Engine and Vehicle Standards and Highway Fuel Sulfur Control Requirements, Regulatory Announcement, EPA420-F-00-057, December 2000, http://www.epa.gov/oms/highway-diesel/regs/f00057.pdf.
[2] J.T. Sampanthar, H. Xiao, J. Dou, T.Y. Nah, R. Xu, P.K. Wong, A novel oxidative desulfurization process to remove refractory sulfur compounds from diesel fuel, Appl. Catal. B: Environ. 63 (2006) 85–93.
[3] A. Takahashi, F.H. Yang, R.T. Yang, New sorbents for desulfurization by π-complexation: thiophene/benzene adsorption, Ind. Eng. Chem. Res. 41 (2002) 2487–2496.
[4] R.T. Yang, A.J. Hernandez-Maldonado, F.H. Yang, Desulfurization of transportation fuels with zeolites under ambient conditions, Science 301 (2003) 79–81.
[5] A.J. Hernandez-Maldonado, R.T. Yang, New sorbents for desulfurization of diesel fuels via π-complexation, AIChE J. 50 (2004) 791–801.
[6] W. Dai, Y.P. Zhou, S.N. Li, W. Li, W. Su, Y. Sun, L. Zhou, Thiophene capture with complex adsorbent SBA-15/Cu (I), Ind. Eng. Chem. Res. 45 (2006) 7892–7896.
[7] A.J. Hernandez-Maldonado, G.S. Qi, R.T. Yang, Desulfurization of commercial fuels by π-complexation: monolayer CuCl/γ-$Al_2O_3$, Appl. Catal. B: Environ. 61 (2005) 212–218.
[8] J.H. Kim, X.L. Ma, A.N. Zhou, C. Song, Ultra-deep desulfurization and denitrogenation of diesel fuel by selective adsorption over three different adsorbents: a study on adsorptive selectivity and mechanism, Catal. Today 111 (2006) 74–83.
[9] A.N. Zhou, X.L. Ma, C. Song, Liquid-phase adsorption of multi-ring thiophenic sulfur compounds on carbon materials with different surface properties, J. Phys. Chem. B 110 (2006) 4699–4707.
[10] Z.X. Jiang, Y. Liu, X.P. Sun, F.P. Tian, F.X. Sun, C.H. Liang, W.S. You, C.R. Han, C. Li, Activated carbons chemically modified by concentrated $H_2SO_4$ for the adsorption of the pollutants from wastewater and dibenzothiophene from fuel oils, Langmuir 19 (2003) 731–736.
[11] Y.X. Yang, H.Y. Liu, P.L. Ying, Z.X. Jiang, C. Li, Selective dibenzothiophene adsorption on modified activated carbons, Carbon 45 (2007) 3042–3044.
[12] Y. Sano, K.H. Choi, Y. Korai, I. Mochida, Adsorptive removal of sulfur and nitrogen species from a straight run gas oil over activated carbons for its deep hydrodesulfurization, Appl. Catal. B: Environ. 49 (2004) 219–225.
[13] A.J. Hernández-Maldonado, R.T. Yang, Desulfurization of commercial liquid fuels by selective adsorption via π-complexation with Cu (I)-Y Zeolite, Ind. Eng. Chem. Res. 42 (2003) 3103–3110.
[14] C. Song, X.L. Ma, New Design approaches to ultra-clean diesel fuels by deep desulfurization and deep dearomatization, Appl. Catal. B: Environ. 41 (2003) 207–238.
[15] G.P. Khare, Desulfurization and novel sorbents for same, US patent 6346190 (2002).
[16] R.L. Irvine, Process for desulfurizing gasoline and hydrocarbon feedstock, US patent 5730860 (1998).
[17] G.X. Yu, S.X. Lu, H. Chen, Z.N. Zhu, Diesel fuel desulfurization with hydrogen peroxide promoted by formic acid and catalyzed by activated carbon, Carbon 43 (2005) 2285–2294.
[18] C.O. Ania, T.J. Bandosz, Importance of structural and chemical heterogeneity of activated carbon surfaces for adsorption of dibenzothiophene, Langmuir 21 (2005) 7752–7759.
[19] Z. Hu, M.P. Srinivasan, Y. Ni, Preparation of mesoporous high-surface-area activated carbon, Adv. Mater. 12 (2000) 62–65.
[20] C. Pelekani, V.L. Snoeyink, Competitive adsorption between atrazine and methylene blue on activated carbon: the importance of pore size distribution, Carbon 38 (2000) 1423–1436.
[21] C. Pelekani, V.L. Snoeyink, A kinetic and equilibrium study of competitive adsorption between atrazine and Congo red dye on activated carbon: the importance of pore size distribution, Carbon 39 (2001) 25–37.
[22] C.T. Hsieh, H.S. Teng, Influence of mesopore volume and adsorbate size on adsorption capacities of activated carbons in aqueous solutions, Carbon 38 (2000) 863–869.
[23] M. Almarri, X.L. Ma, C. Song, Selective adsorption for removal of nitrogen compounds from liquid hydrocarbon streams over carbon- and alumina-based adsorbents, Ind. Eng. Chem. Res. 48 (2009) 951–960.
[24] Y. Sano, K.H. Choi, Y. Korai, I. Mochida, Selection and further activation of activated carbons for removal of nitrogen species in gas oil as a pretreatment for its deep hydrodesulfurization, Energy Fuels 18 (2004) 644–651.
[25] X.L. Ma, K.Y. Sakanishi, I. Mochida, Hydrodesulfurization reactivities of various sulfur-compounds in diesel fuel, Ind. Eng. Chem. Res. 33 (1994) 218–222.
[26] F.Y. Liang, M.M. Lu, M. Eileen Birch, T.C. Keener, Z.F. Liu, Determination of polycyclic aromatic sulfur heterocycles in diesel particulate matter and diesel fuel by gas chromatography with atomic emission detection, J. Chromatogr. A 1114 (2006) 145–153.
[27] C. Song, Chemistry of Diesel Fuels, 1st Ed., CRC, New York, 2000.
[28] F.L. Tungate, D. Hopkins, D.C. Huang, J. Fletcher, E. Kohler, Advanced distillate hydroprocessing ASAT, a trifunctional HDAR/HDS/HDN catalyst, In: NPRA 1999 Annual Meeting, San Antonio, Texas, 1999, Paper AM-99-38.
[29] C. Valderrama, X. Gamisans, X. de las Heras, A. Farran, J.L. Cortina, Sorption kinetics of polycyclic aromatic hydrocarbons removal using granular activated carbon: intraparticle diffusion coefficients, J. Hazard. Mater. 157 (2008) 386–396.
[30] Y.P. Guo, S. Kaplan, T. Karanfil, The significance of physical factors on the adsorption of polyaromatic compounds by activated carbons, Carbon 46 (2008) 1885–1891.
[31] C.O. Ania, B. Cabal, C. Pevida, A. Arenillas, J.B. Parra, F. Rubiera, J.J. Pis, Effects of activated carbon properties on the adsorption of naphthalene from aqueous solutions, Appl. Surf. Sci. 253 (2007) 5741–5746.
[32] R.W. Walters, R.G. Luthy, Equilibrium adsorption of polycyclic aromatic hydrocarbons from water onto activated carbon, Environ. Sci. Technol. 18 (1984) 395–403.
[33] A.M. Dowaidar, M.S. EI-Shahawi, I. Ashour, Adsorption of polycyclic aromatic hydrocarbons onto activated carbon from non-aqueous media: 1. The influence of the organic solvent polarity, Sep. Sci. Technol. 42 (2007) 3609–3622.
[34] Z.Q. Gong, K. Alef, B.M. Wilke, P.J. Li, Activated carbon adsorption of PAHs from vegetable oil used in soil remediation, J. Hazard. Mater. 143 (2007) 372–378.
[35] F.B. Su, L. Lv, T.M. Hui, X.S. Zhao, Phenol adsorption on zeolite-templated carbons with different structural and surface properties, Carbon 43 (2005) 1156–1164.
[36] T.H. Nguyen, H.H. Cho, D.L. Poster, W.P. Ball, Evidence for a pore-filling mechanism in the adsorption of aromatic hydrocarbons to a natural wood char, Environ. Sci. Technol. 41 (2007) 1212–1217.
[37] C. Yu, J.S. Qiu, Y.F. Sun, X.H. Li, G. Chen, Z. Bin, Adsorption removal of thiophene and dibenzothiophene from oils with activated carbon as adsorbent: effect of surface chemistry, J. Porous Mater. 15 (2008) 151–157.
[38] Y.F. Jia, K.M. Thomas, Adsorption of cadmium ions on oxygen surface sites in activated carbon, Langmuir 16 (2000) 1114–1122.
[39] S. Biniak, G. Szymanski, J. Siedlewski, A. Swiatkowski, The characterization of activated carbons with oxygen and nitrogen surface groups, Carbon 35 (1997) 1799–1810.
[40] D. Jayne, Y. Zhang, S. Haji, C. Erkey, Dynamics of removal of organosulfur compounds from diesel by adsorption on carbon aerogels for fuel cell applications, Int. J. Hydrogen Energy 30 (2005) 1287–1293.
[41] T. Garcia, R. Murillo, D. Cazorla-Amoros, A.M. Mastral, A. Linares-Solano, Role of the activated carbon surface chemistry in the adsorption of phenanthrene, Carbon 42 (2004) 1683–1689.
[42] R. Murillo, T. Garcia, E. Aylon, M.S. Callen, M.V. Navarro, J.M. Lopez, A.M. Mastral, Adsorption of phenanthrene on activated carbons: breakthrough curve modelling, Carbon 42 (2004) 2009–2017.

[43] M.A. Lillo-Rodenas, D. Cazorla-Amoros, A. Linares-Solano, Behaviour of activated carbons with different pore size distributions and surface oxygen groups for benzene and toluene adsorption at low concentrations, Carbon 43 (2005) 1758–1767.
[44] H. Soscun, Y. Alvarado, J. Hernandez, P. Hernandez, R. Atencio, A. Hinchliffe, Experimental and theoretical determination of the dipole polarizability of dibenzothiophene, J. Phys. Org. Chem. 14 (2001) 709–715.
[45] M. Daage, R.R. Chianelli, Structure-function relations in molybdenum sulfide Catalysts: the "Rim-Edge" model, J. Catal. 149 (1994) 414–427.
[46] V. Meille, E. Schulz, M. Lemaire, R. Faure, M. Vrina, An efficient synthesis of pure 4,6-dimethyldibenzothiophene, Tetrahedron 52 (1996) 3953–3960.
[47] L. Sutton, Tables of interatomic distances and configuration in molecules and ions, Chemical Society London, Chemical Society, 1958.
[48] L.C. Sander, S.A. Wise, Polycyclic Aromatic hydrocarbon structure index, NIST Special Publication 922, http://www.cstl.nist.gov/acd/839.02/pah/alpha.htm.
[49] M.M. Dubinin, in: P.L. Walker (Ed.), Chemistry and Physics of Carbon, Vol. 2, Marcel Dekker, New York, 1966, p. p. 51.
[50] P.A. Quinlivan, L. Li, D.R.U. Knappe, Effects of activated carbon characteristics on the simultaneous adsorption of aqueous organic micropollutants and natural organic matter, Water Res. 39 (2005) 1663–1673.
[51] C.N. Satterfield, C.K. Colton, W.H. Pitcher Jr, Restricted diffusion in liquids within fine pores, AIChE J. 119 (973) (2005) 628–635.
[52] A. Chantong, F.E. Massoth, Restrictive diffusion in aluminas, AIChE J. 29 (1983) 725–731.
[53] M. Seredych, E. Deliyanni, T.J. Bandosz, Role of microporosity and surface chemistry in adsorption of 4,6-dimethyldibenzothiophene on polymer-derived activated carbons, Fuel 89 (2010) 1499–1507.
[54] Y.M. Wu, A. Borgna, PCT Patent Application WO/2009/099395A1.
[55] A. Borgna, J. Bu, C.G. Gwie, G. Loh, S. Dewiyanti, US Provisional Patent Application No. 61/333,40 (2010).